Archives of Oral Biology 155 (2023) 105797

Contents lists available at ScienceDirect

Archives of Oral Biology

journal homepage: www.elsevier.com/locate/archoralbio

Ruxolitinib altered IFN-β induced necroptosis of human dental pulp stem cells during osteoblast differentiation

Atsuko Tanaka [a], Satoru Hayano [a,*], Masayo Nagata [b], Takahiro Kosami [b], Ziyi Wang [c,d], Hiroshi Kamioka [b]

[a] Department of Orthodontics, Okayama University Hospital, Okayama, Japan
[b] Department of Orthodontics, Graduate School of Medicine, Dentistry and Pharmaceutical Sciences, Okayama University, Okayama, Japan
[c] Department of Molecular Biology and Biochemistry, Okayama University Graduate School of Medicine, Dentistry and Pharmaceutical Sciences, Okayama, Japan
[d] Research Fellow of Japan Society for the Promotion of Science, Tokyo, Japan

ARTICLE INFO

Keywords:
Type-I interferon
Janus kinase/signal transducers and activators of transcription pathway
Osteoblast
Necroptosis
Singleton-Merten Syndrome

ABSTRACT

Objective: This study aimed to evaluate the role of ruxolitinib in the interferon beta (IFN-β) mediated osteoblast differentiation using human dental pulp stem cells (hDPSCs).
Design: hDPSCs from five deciduous teeth of healthy patients were stimulated by adding human recombinant IFN-β protein (1 or 2 ng/ml) to the osteogenic differentiation induction medium. Substrate formation was determined using Alizarin Red staining, calcium concentration, and osteoblast marker expression levels. Ruxolitinib was used to inhibit the Janus kinase/signal transducers and activators of transcription (JAK-STAT) pathway. Apoptosis was detected using terminal deoxynucleotidyl nick-end labeling (TUNEL) staining, and necroptosis was detected using propidium iodide staining and phosphorylated mixed lineage kinase domain-like protein (pMLKL) expression.
Results: In the IFN-β-treated group, substrate formation was inhibited by a reduction in alkaline phosphatase (*ALP*) expression in a concentration-dependent manner. Although the proliferation potency was unchanged between the IFN-β-treated and control groups, the cell number was significantly reduced in the experimental group. TUNEL-positive cell number was not significantly different; however, the protein level of necroptosis markers, interleukin-6 (*IL-6*) and pMLKL were significantly increased in the substrate formation. Cell number and *ALP* expression level were improved in the group administered ruxolitinib, a JAK-STAT inhibitor. Additionally, ruxolitinib significantly suppressed *IL-6* and pMLKL levels.
Conclusion: Ruxolitinib interfered with the IFN-β-mediated necroptosis and osteogenic differentiation via the JAK-STAT pathway.

1. Introduction

Recently, a case report has shown that administration of ruxolitinib improved bone mineralization in a Singleton-Merten Syndrome (SMS [MIM 182250]) patient (Broser et al., 2022); however, the molecular mechanism is still unknown. SMS is a rare autosomal dominant congenital disease characterized by autoimmune diseases and dentoskeletal abnormalities including severe root and alveolar bone resorption. SMS, as a kind of type I interferonopathies, is caused by gain-of-function mutations in the interferon induced with helicase C domain 1 (*IFIH1*) gene, which eventually results in overactivation of type I interferon (IFN-β) signaling leading to autoinflammation mainly

Abbreviation: IFN type I, type I interferon; RANKL, receptor activator of nuclear factor-κB ligand; ISGs, interferon-stimulated genes; JAK-STAT, Janus kinase/signal transducers and activators of transcription; pMLKL, phosphorylated mixed lineage kinase domain-like protein; SMS, Singleton-Merten Syndrome; DPSC, dental pulp stem cell; hDPSC, human dental pulp stem cell; DMEM, Dulbecco's modified Eagle's medium; HIFBS, heat-inactivated fetal bovine serum; α-MEM, alpha medium; AR, Alizarin Red; RT-qPCR, reverse transcription PCR; cDNA, complementary DNA; TUNEL, terminal deoxynucleotidyl nick-end labeling; DAPI4', 6-diamidino-2-phenylindole; RIPA, radioimmunoprecipitation; BCA, bicinchoninic; SDS-PAGE, sodium dodecyl sulfate-polyacrylamide gel electrophoresis; PVDF, polyvinylidene fluoride; TBS-T, tris-buffered saline with tween; GAPDH, glyceraldehyde-3-phosphate dehydrogenase; HRP, horseradish peroxidase; SD, standard deviation; BSP, bone sialoprotein; *CASP9*, Caspase 9; PI, propidium iodide; *IL-6*, interleukin-6.

* Correspondence to: Department of Orthodontics, Okayama University Hospital, 2-5-1 Shikatacho, Kita-ku, Okayama 700-8525, Japan.
E-mail address: shayano@okayama-u.ac.jp (S. Hayano).

https://doi.org/10.1016/j.archoralbio.2023.105797
Received 20 February 2023; Received in revised form 1 August 2023; Accepted 21 August 2023
Available online 22 August 2023

through the Janus kinase/signal transducers and activators of transcription (JAK-STAT) pathway (Andzinski et al., 2015; Lu & MacDougall, 2017; Pettersson et al., 2017; Rice et al., 2020; Rutsch et al., 2015; Takaoka et al., 2003). Ruxolitinib, as a JAK inhibitor, was approved for medical use in the United States in 2011, and in the European Union in 2012 for the treatment of disease-related splenomegaly or symptoms in adults with primary myelofibrosis (also known as chronic idiopathic myelofibrosis), post-polycythaemia-vera myelofibrosis, or post-essential thrombocythaemia myelofibrosis (O'Shea et al., 2015).

Although IFN-β has been reported to induce bone formation by reducing c-Fos expression during receptor activator of nuclear factor-κB ligand (RANKL)-induced osteoclastogenesis (Amarasekara et al., 2018; Takayanagi et al., 2002), there are few studies have been reported about the effects of IFN-β on osteoblastogenesis. IFN type I is a general term for the interferon family, which includes IFN-α and IFN-β, and plays a major role in antiviral activity (de Weerd et al., 2013; Ikushima et al., 2013; Ivashkiv & Donlin, 2014; Piehler et al., 2012; Wittling et al., 2021). IFN type I induces type I interferon-stimulated genes (ISGs) via JAK-STAT pathway, and ISGs induce p53, an apoptosis-inducing protein. These findings suggested that IFN type I induces apoptosis (Andzinski et al., 2015; Porta et al., 2005; Takaoka et al., 2003).

Apoptosis is a programmed cell death that does not induce an inflammatory response (Haanen & Vermes, 1995) and is regulated by caspases, a family of cysteine proteases. Apoptosis can be triggered by executive caspases (Caspase-3, 7), which are cleaved by initiator caspases (Caspase-2, 8, 9) (Li et al., 2017; Shakeri et al., 2017; Shi, 2002; Xu et al., 2019). Cell death has been classified into apoptosis, an active cell death regulated by molecules, and necrosis, a passive cell death not regulated by molecules (Schwartz & Osborne, 1993). However, recent studies have identified new types of necroses associated with inflammatory responses and controlled by molecules (D'arcy, 2019; Nikoletopoulou et al., 2013; Su et al., 2015). Among them, necroptosis is a programmed cell death triggered by phosphorylated mixed lineage kinase domain-like protein (pMLKL). Moreover, IFN type I activates the phosphorylation of MLKL via the JAK-STAT pathway (Huang et al., 2012; Liu et al., 2019; McComb et al., 2014; Sarhan et al., 2019).

Although the effects of IFN type I on osteoblasts have not been elucidated, it causes cell death via the JAK-STAT pathway in tumor cells (Andzinski et al., 2015; Huang et al., 2012; Liu et al., 2019; McComb et al., 2014; Porta et al., 2005; Sarhan et al., 2019; Takaoka et al., 2003). Therefore, it was speculated that increased IFN type I may suppress osteoblast function. In fact, osteoporotic phenotypes are reported in diseases associated with the increased expression of ISGs, which are collectively referred to as type I interferonopathies (Briggs et al., 2011).

As mentioned above, the JAK-STAT might be profoundly involved in the IFN-β-mediated bone metabolism via regulating cell apoptosis or necroptosis; while the role of JAK inhibitor, ruxolitinib, in the IFN-β-mediated bone metabolism has been poorly reported. Therefore, in this study, the JAK-STAT dependent effect of IFN-β on osteoblasts was investigated by adding IFN-β recombinant protein to the human dental pulp stem cell (hDPSCs) osteogenic differentiation induction medium with/without ruxolitinib. IFN-β induced necroptosis in the differentiating osteoblasts; however, this effect was partially neutralized by a ruxolitinib. This study presents the first molecular evidence of the role of IFN type I during osteoblastogenesis, which is beneficial for the pharmacological treatment of patients with type I interferonopathies.

2. Materials and methods

2.1. Study approval

The study protocol was approved by the institutional ethics committee of Okayama University (approval number 1701–024). Informed consent was obtained from all participants prior to their participation in the study.

Table 1
Primers for reverse transcription-polymerase chain reaction.

Primer	Direction	Sequence
GAPDH	forward	5'-GACAAGCTTCCCGTTCTCAG-3'
	reverse	5'-CAATGACCCCTTCATTGACC-3'
ALP	forward	5'-GTGGAAGGAGGCAGAATTGA-3'
	reverse	5'-AGACTGCGCCTGGTAGTTGT-3'
Osteocalcin	forward	5'-AGAGTCCAGCAAAGGTGCAG-3'
	reverse	5'-TCAGCCAACTCGTCACAGTC-3'
BSP	forward	5'-TCACTGGAGCCAATGCAGAA-3'
	reverse	5'-TGGAGAGGTTGTTGTCTTCGAG-3'
CASP9	forward	5'-GGTACGTTGAGACCCTGGAC-3'
	reverse	5'-CACCGAAACAGCATTAGCGAC-3'
IL6	forward	5'-CTGGAGGTACTCTAGGTATAC-3'
	reverse	5'-GTGTGAAAGCAGCAAAGAGGC-3'

2.2. Isolation and culture of human dental pulp stem cells

Five deciduous teeth were extracted from healthy patients who ranged in age from 8 years 1 month to 11 years 1 month (average age 10.0 years) undergoing orthodontic treatment at the Okayama University Hospital. Dental pulp was isolated from five extracted deciduous teeth according to previous studies (Gronthos et al., 2000; Kawanabe et al., 2015; Miura et al., 2003). The isolated pulp tissues were subjected to enzymatic digestion using a mixture of low-glucose Dulbecco's modified Eagle's medium (DMEM) (Invitrogen, Carlsbad, CA, USA) supplemented with 5 mg/ml collagenase type II (Worthington, Lakewood, NJ, USA) and 2.5 mg/ml dispase I (Roche, Penzberg, Germany) for 60 min at 37 ℃. The isolated hDPSCs were maintained in low-glucose DMEM supplemented with 10 % heat-inactivated fetal bovine serum (HIFBS) (HyClone, Logan, UT, USA) and penicillin/streptomycin (100 U/ml and 10 mg/ml, respectively; Invitrogen). The medium was changed once a week. The primary cultured cells were used for experiments after undergoing two times of passage. We have previously demonstrated that cells purified by these methods are stem cells which can differentiate into osteoblasts, chondrocytes, and adipocytes (Kawanabe et al., 2012).

2.3. Osteoblast differentiation

For osteoblast differentiation, human DPSCs (hDPSCs) were cultured in the presence of alpha medium (α-MEM) (Invitrogen) containing 10 % HIFBS, penicillin/streptomycin, 100 nM dexamethasone, 0.05 mM L-ascorbic acid (Sigma), and 10 mM β-glycerophosphate (Sigma) for 2 weeks. Cells were maintained by changing the medium every 3–4 d. Osteoblast differentiation was characterized using Alizarin Red (AR) S staining (1 mg/ml; Nacalai Tesque, Kyoto, Japan) and Calcium E-test WAKO (FUJIFILM Wako, Osaka, Japan).

2.4. Treatment of hDPSCs with IFN-β recombinant protein and ruxolitinib

IFN-β recombinant protein (HZ-1298, Proteintech, IL, USA) was added to the hDPSC osteoblastic differentiation induction medium. The concentration of IFN-β was decided by cell viability assay. Next, ruxolitinib (1 mM; ab141356, Abcam, Cambridge, UK) was added as an inhibitor of the JAK-STAT pathway. The concentration of ruxolitinib was decided based on a previous study (Qian et al., 2022).

2.5. Reverse transcription-quantitative polymerase chain reaction

Total RNA was isolated using the RNeasy Mini Kit (Qiagen, Hilden, Germany) according to the manufacturer's protocol. Reverse transcription PCR (RT-qPCR) was performed using ReverTra Ace qPCR RT Kit (Toyobo, Osaka, Japan) by heating at 37 ℃ for 15 min and enzyme deactivation at 98 ℃ for 5 min. Complementary DNA (cDNA) was analyzed using qPCR using gene-specific primers and SYBR Green PCR Master Mix (Toyobo). The relative levels of the PCR products were

assessed using a LightCycler System (Roche Diagnostics, Mannheim, Germany). Glyceraldehyde-3-phosphate dehydrogenase (GAPDH) was used as an endogenous reference gene. The primer sequences used are listed in Table 1.

2.6. TUNEL assay and immunofluorescence

After 14 days of culture, differentiated osteoblasts were fixed in 4 % paraformaldehyde (Nacalai Tesque) at room temperature for 15 min. DNA fragmentation was measured using the terminal deoxynucleotidyl nick-end labeling (TUNEL) In Situ Cell Death Detection Kit, Fluorescein (Roche Applied Bioscience), according to the manufacturer's instructions. Proliferation-associated nuclear antigens in fixed osteoblasts were detected using an Anti-Ki67 antibody (1:250; ab16667, Abcam). Goat anti-rabbit IgG (H+L) Cross-Adsorbed Secondary Antibody, Alexa Fluor488, was used as the secondary antibody. Cells were washed with phosphate-buffered saline (PBS), and nuclei were stained using 4',6-diamidino-2-phenylindole (DAPI) (1:1000; D9542, Sigma) for 10 min at room temperature. Fluorescent images were processed using the ImageJ software (NIH, Bethesda, MD, USA).

2.7. PI staining

After 14 days of culture, differentiated osteoblasts were stained using the Apoptotic & Necrotic & Healthy Cells Quantification Kit (Biotium Inc., Hayward, CA, USA) according to the manufacturer's instructions. Fluorescent images were processed using ImageJ software.

2.8. Western blotting analysis

After washing the cultured osteoblasts with cold PBS, the cells were lysed using radioimmunoprecipitation (RIPA) lysis buffer (Merck, Darmstadt, Germany) containing 0.1 % Halt Protease and Phosphatase Inhibitor (Thermo Fisher Scientific, Waltham, MA, USA). The amount of protein was quantified using a bicinchoninic (BCA) protein assay kit (Thermo Fisher Scientific) and was adjusted to 40 mg per lane. Each sample was separated using sodium dodecyl sulfate-polyacrylamide gel electrophoresis (SDS-PAGE) and transferred onto a polyvinylidene fluoride (PVDF) membrane. The transferred membrane was blocked with 5 % skimmed milk in tris-buffered saline with tween (TBS-T) at 4 ℃ for 60 min and incubated overnight with the primary antibody pMLKL (1:1000; #91689, Cell Signaling Technology, MA, USA). GAPDH (1:1000; #2118, Cell Signaling Technology) was used as the loading control. After overnight incubation, the membrane was thoroughly washed and reacted with a secondary antibody, anti-rabbit IgG, horseradish peroxidase (HRP)-linked antibody (1:1000; #7074, Cell Signaling Technology) at 20 ℃ for 1 h. The bound antibody was detected using a 20X LumiGLO chemiluminescence system (ChemiDoc™ XRS+; Bio-Rad, Berkeley, Calif., USA).

2.9. Statistical analyses

All quantified results are expressed as the mean ± standard deviation (SD) of five biological replicates indicated by the scattered points in the bar charts, and each biological replicate was measured with two or three technical replicates. The Shapiro-Wilk test was performed to test the normality of all results with $\alpha = 0.01$ (Supplemental Table 1). Since the two-way analysis of variance (ANOVA) is considered "robust" to violations of normality (Blanca et al., 2017; Islam & Abbas, 2022) and all of our data are approximately normality (P-values > 0.01 by Shapiro-Wilk test in Supplemental Table 1), an ordinary two-way ANOVA ($\alpha = 0.05$), followed by a Tukey's multiple comparison with a single pooled variance ($\alpha = 0.05$), was performed for the results with more than two groups. Given that nonparametric tests are often a good option for the small sample size ($n < 30$), Mann-Whitney test with $\alpha = 0.05$ was applied for the results with only two groups (Kaur & Kumar, 2015). All

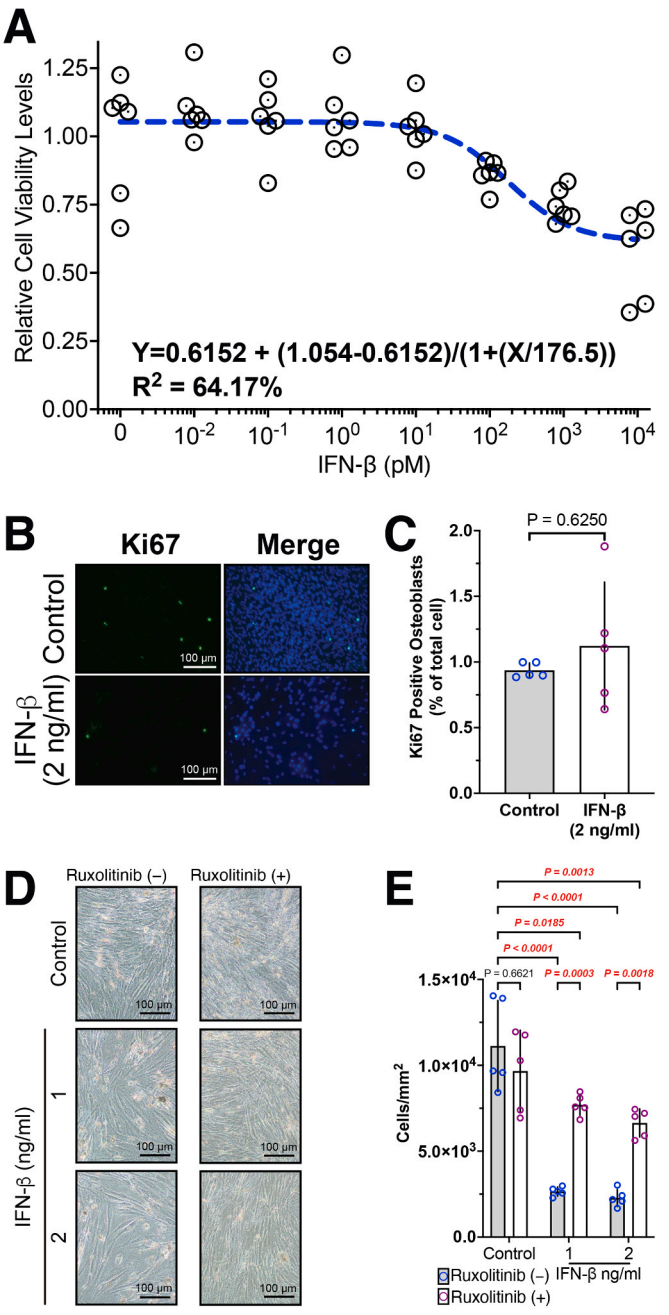

Fig. 1. IFN-β mediated proliferation of human dental pulp stem cells independent of Ki67.
(**A**) Toxicity test of IFN-β on human dental pulp stem cells (hDPSCs). (**B**) Detection of proliferating osteoblasts using immunocytochemistry using Ki67 (green). Nuclei stained with 4',6-diamidino-2-phenylindole (DAPI) (blue). (**C**) Quantification of Ki67-positive cells in the control and IFN-β-treated groups. (**D**, **E**) Representative transmitted light image (**D**) and cell number (**E**) of induced osteoblasts in the control and IFN-β-treated groups with/whithout ruxolitinib. All quantified results above are presented as the mean ± standard deviation (SD) with scattered points shown each biological replicate.

Table 2
Two-way ANOVA details for Figs. 1E, 2B-E, and 3D-E.

	Source of Variation	Sum of Squares	df	Mean Square	F	*P*-value	Percentage of total variation (%)
Dependent Variable:	Interaction (IFN-β × Ruxolitinib)	63955895	2	31977948	13.66	***0.0001***	16.72
Cells/mm^2	IFN-β	209794180	2	104897090	44.81	< ***0.0001***	54.83
	Ruxolitinib	52688627	1	52688627	22.51	< ***0.0001***	13.77
	Residual	56178715	24	2340780			
Dependent Variable:	Interaction (IFN-β × Ruxolitinib)	500.60	2	250.3	4.16	***0.0282***	7.95
Normalized Calcium	IFN-β	4297.00	2	2149	35.69	< ***0.0001***	68.22
Concentration (mg/dl)	Ruxolitinib	56.51	1	56.51	0.94	0.3423	0.90
	Residual	1445.00	24	60.20			
Dependent Variable:	Interaction (IFN-β × Ruxolitinib)	0.29	2	0.15	3.82	***0.0363***	7.04
ALP/GAPDH	IFN-β	2.28	2	1.14	29.95	< ***0.0001***	55.17
(mRNA)	Ruxolitinib	0.65	1	0.65	17.04	***0.0004***	15.69
	Residual	0.91	24	0.04			
Dependent Variable:	Interaction (IFN-β × Ruxolitinib)	1.43	2	0.72	3.56	***0.0444***	14.09
Osteocalcin/GAPDH	IFN-β	2.19	2	1.10	5.43	***0.0113***	21.53
(mRNA)	Ruxolitinib	1.71	1	1.71	8.51	***0.0076***	16.85
	Residual	4.84	24	0.20			
Dependent Variable:	Interaction (IFN-β × Ruxolitinib)	0.01	2	0.00	0.03	0.9735	0.19
BSP/GAPDH	IFN-β	0.67	2	0.33	1.79	0.1880	12.90
(mRNA)	Ruxolitinib	0.03	1	0.03	0.16	0.6890	0.59
	Residual	4.46	24	0.19			
Dependent Variable:	Interaction (IFN-β × Ruxolitinib)	0.04	2	0.02	1.19	0.3207	2.90
CASP9/GAPDH	IFN-β	0.96	2	0.48	26.11	< ***0.0001***	63.53
(mRNA)	Ruxolitinib	0.07	1	0.07	3.60	0.0701	4.37
	Residual	0.44	24	0.02			
Dependent Variable:	Interaction (IFN-β × Ruxolitinib)	178.40	2	89.20	24.20	< ***0.0001***	19.29
IL-6/GAPDH	IFN-β	301.20	2	150.60	40.86	< ***0.0001***	32.57
(mRNA)	Ruxolitinib	356.80	1	356.80	96.81	< ***0.0001***	38.58
	Residual	88.45	24	3.69			

ANOVA, analysis of variance; **df**, degrees of freedom; α = 0.05.

statistical analyses were performed using GraphPad Prism 8 for Windows.

3. Results

3.1. IFN-β mediated proliferation of human dental pulp stem cells independent of Ki67

We performed the toxicity test of IFN-β to determine the largest concentration that keeps high cell viability (>90 % of the control group). According to the dose-response curve from Fig. 1A, the concentration of ruxolitinib at 50 and 100 pM (1 and 2 ng/ml) will result in 96 % and 90 % viability compared with the control group. We, therefore, used this concentration in all the following experiments.

Although the percentage of Ki67-positive proliferating hDPSCs was not significantly changed by treatment with 2 ng/ml of IFN-β compared with the control group (Fig. 1B and C), the cell numbers were significantly reduced by IFN-β at both 1 and 2 ng/ml levels (Figs. 1D and 1E). Moreover, ruxolitinib ameliorated the IFN-β-decreased cell number (Figs. 1D and 1E) and showed a significant interaction effect with IFN-β (Table 2). The interaction effect between ruxolitinib and IFN-β on the cells number contributes a higher percentage of variation compared with ruxolitinib alone (16.72 % v.s. 13.77 % in Table 2), and cells number has unchanged with ruxolitinib treatment only (Fig. 1E). Thus, the ruxolitinib can impact the cell proliferation only when combined with IFN-β.

Those findings indicated that IFN-β-mediated proliferation of hDPSCs during osteoblast differentiation was partially reliant on the JAK-STAT pathway but independent from Ki67.

3.2. Ruxolitinib interfered with the IFN-β-mediated osteoblastogenesis

To determine the effects of IFN-β on osteoblast differentiation of hDPSCs, undifferentiated mesenchymal stem cells, isolated from extracted dental pulp from healthy patients, were evaluated for their differentiation into osteoblasts. AR staining was performed after 14 days of culture in the osteoblastic differentiation induction medium to compare mineralization rates. In the IFN-β-treated groups, calcification was inhibited in a concentration-dependent manner (Fig. 2A). In addition, calcium concentration (normalized to the cells number from Fig. 1E) in the culture medium was lower in the IFN-β group than in the control group (Fig. 2B).

Although ruxolitinib in the IFN-β group did not induce statistically significant changes (Fig. 2B), the interaction effect between ruxolitinib and IFN-β on calcium concentration was significant and contributed 7.95 % of total variation (Table 2). Additionally, decreased amount of calcium concentration was reduced in IFN-β with ruxolitinib compared with IFN-β treatment only (Fig. 2B). Compared to the control group, 2 ng/ml IFN-β reduced approximately 98 % of calcium concentration with a *P*-value smaller than 0.0001, while 2 ng/ml IFN-β combined with ruxolitinib only reduced about 66 % of calcium concentration with *P*-value of 0.0002 (Fig. 2B).

Meanwhile (Fig. 2C-E), IFN-β significantly decreased the expression of ALP, an early-stage osteoblastic differentiation maker (Amarasekara et al., 2021); and increased the expression of osteocalcin, a mature osteoblastic differentiation marker (Amarasekara et al., 2021). Since osteoblast differentiation requires a sophisticated balance and changes among different critical differentiation markers (Amarasekara et al., 2021; Karsenty et al., 2009; Liao et al., 2022), IFN-β treatment interfered with the osteoblast differentiation of hDPSCs via *ALP* and *osteocalcin* but not *BSP* (Fig. 2C-E). Those findings were consistence with AR staining results (Fig. 2A).

Interestingly, adding ruxolitinib into the 2 ng/ml IFN-β treatment group rescued the IFN-β-impacted expression of *ALP* and *osteocalcin* (Fig. 2C and D). Ruxolitinib with 2 ng/ml IFN-β increased the IFN-β-reduced expression of ALP and decreased the IFN-β-promoted-osteocalcin back to the level as the same as the control group with the *P*-values of 0.2286 and 0.9966, respectively (Fig. 2C and D).

Those findings indicated that ruxolitinib rescued the IFN-β-impaired osteoblast differentiation, consistent with the previous case report that administration of ruxolitinib improved bone mineralization in an SMS patient (Broser et al., 2022).

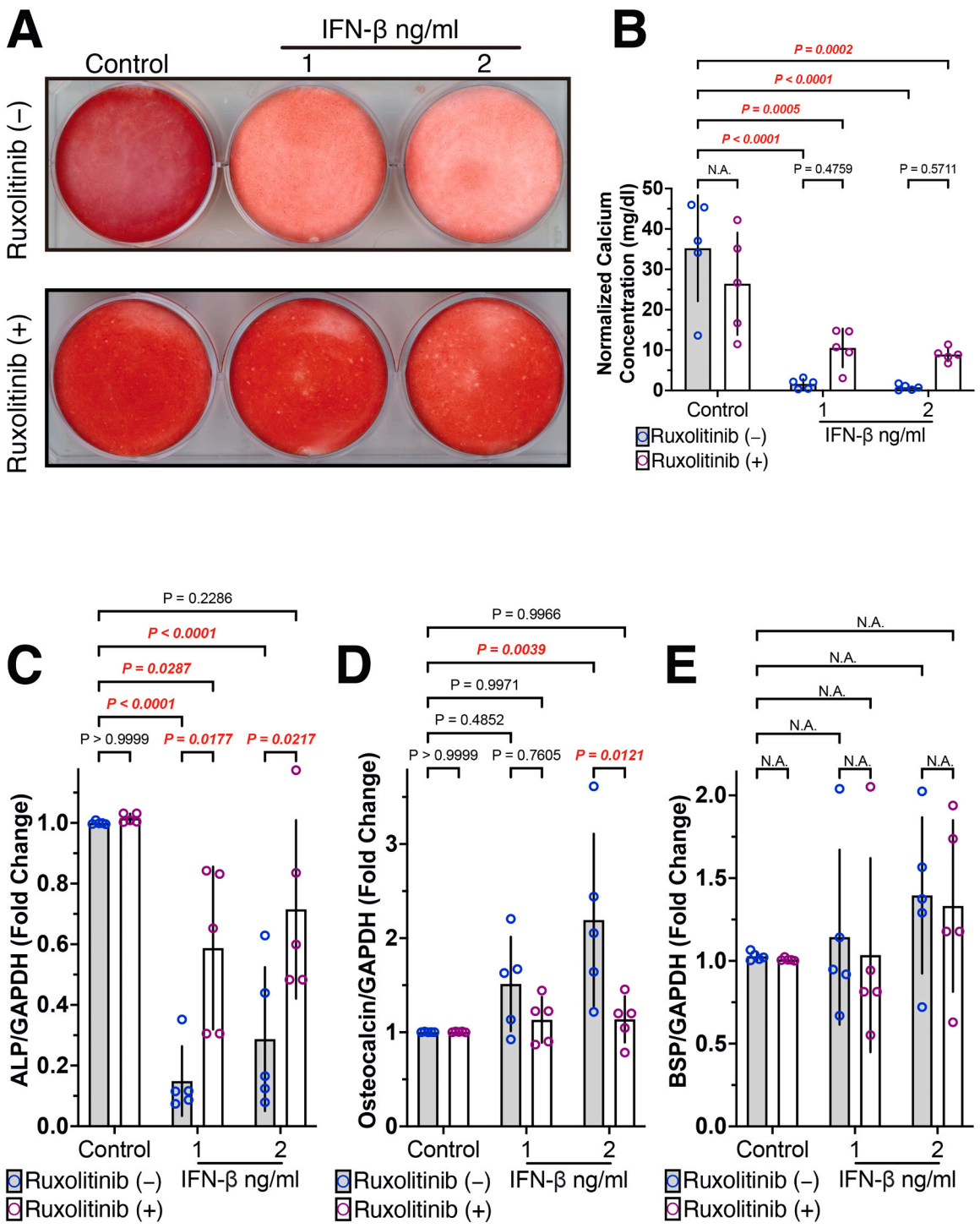

Fig. 2. Ruxolitinib interfered with the IFN-β-mediated osteoblastogenesis. (A, B) Alizarin Red (AR) staining (A) and normalized calcium concentration level (B) of human dental pulp stem cells (hDPSCs) 14 days after osteogenic induction in the control and IFN-β-treated groups with/whithout ruxolitinib. The calcium concentration was normalized using the cells number results from Fig. 1D. (C, D, E) Total RNA isolated from the differentiated osteoblasts and messenger RNA (mRNA) expression levels of (C) alkaline phosphatase (*ALP*), (D) *osteocalcin*, and (E) bone sialoprotein (*BSP*) measured using reverse transcription-quantitative PCR (RT-qPCR) using glyceraldehyde-3-phosphate dehydrogenase (*GAPDH*) as an internal reference. All quantified results above are presented as the mean ± standard deviation (SD) with scattered points shown each biological replicate. N.A., not applicable.

3.3. Ruxolitinib impacted the IFN-β-mediated osteoblast necroptosis

To investigate the role of IFN-β in cell death, DNA fragmentation and gene expression levels associated with cell death were evaluated using TUNEL staining and RT-qPCR, respectively. Although TUNEL-positive cell numbers were not significantly different (Fig. 3A and B), Caspase 9 (*CASP9*), an apoptosis-specific marker (Krajewski et al., 1999), was significantly elevated in the IFN-β-treated groups (Fig. 3C). Moreover, interleukin 6 (*IL-6*), an inflammatory response marker (Kishimoto, 1989), was significantly elevated in the IFN-β-treated group (Fig. 3D). These results indicated that IFN-β induced both apoptosis and the inflammatory response.

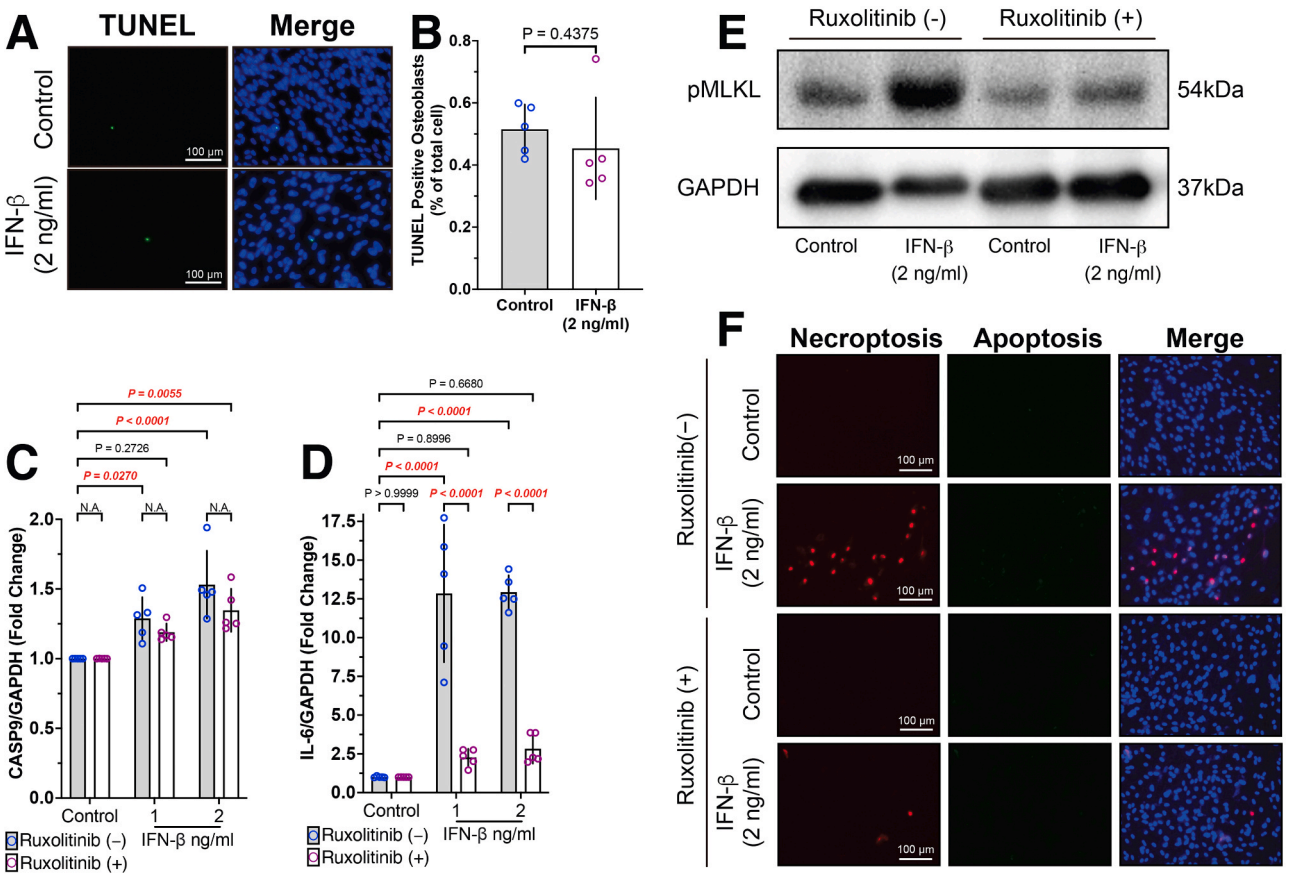

Fig. 3. Ruxolitinib impacted the IFN-β-mediated osteoblast necroptosis. (A) Representative fluorescence image of terminal deoxynucleotidyl nick-end labeling (TUNEL) assay for apoptosis detection. TUNEL-positive nuclei were labeled green, and all nuclei were counterstained with DAPI (blue). (B) Quantification of the apoptotic cells revealed no significant difference between the two groups. (C, D) Total RNA isolated from the differentiated osteoblasts and messenger RNA (mRNA) expression levels of (C) Caspase 9 (*CASPA9*) and (D) interleukin-6 (*IL-6*) measured using reverse transcription-quantitative PCR (RT-qPCR) using glyceraldehyde-3-phosphate dehydrogenase (*GAPDH*) as an internal reference. (E) Western blotting using phosphorylated mixed lineage kinase domain-like protein (pMLKL) antibody. GAPDH was used as a loading control. (F) PI staining images. Red and green indicate necrotic and apoptotic cells, respectively. Nuclei staining are indicated in blue. All quantified results above are presented as the mean ± standard deviation (SD) with scattered points shown each biological replicate. N.A., not applicable.

However, apoptosis normally does not induce inflammatory reaction (Haanen & Vermes, 1995). To determine the relationship between decreased cell number and inflammatory response, the protein levels of pMLKL, an execution factor of necroptosis, were compared. IFN-β significantly increased the pMLKL expression (Fig. 3E). Furthermore, propidium iodide (PI) staining revealed that necroptotic nuclei were dramatically increased in IFN-β-treated osteoblasts (Fig. 3F). Notably, ruxolitinib significantly reduced the IFN-β-increased *IL-6* expression level (Fig. 3D), suppressed the pMLKL production in the IFN-β-treated groups (Fig. 3E), and dramatically decreased the IFN-β-elevated necroptotic nuclei (Fig. 3F). In contrast, both ruxolitinib itself or interaction with IFN-β had no influence on the expression of *CASP9* (Fig. 3C and Table 2).

4. Discussion

Type I interferonopathies are characterized by various clinical manifestations (Crow, 2011; Melki & Frémond, 2020; Munoz et al., 2015; Rice et al., 2014). However, the detailed pathological mechanisms underlying type I interferonopathies have not been clarified, and no definitive treatment has been established. IFN type I has been speculated to induce osteogenesis, given that it inhibits osteoclast differentiation (Amarasekara et al., 2018; Takayanagi et al., 2002). Therefore, it is likely that osteoclastogenesis is suppressed in patients with type I interferonopathie. However, alveolar bone resorption and osteogenesis imperfecta, such as osteoporosis, have been observed in patients with Singleton-Merten Syndrome (SMS [MIM 182250]), which is a representative congenital disease of type I interferonopathie (Lu & MacDougall, 2017; Pettersson et al., 2017; Rice et al., 2020; Rutsch et al., 2015).

Few studies have examined the relationship between IFN type I and osteoblasts or undifferentiated mesenchymal stem cells, and none have used human samples. Melanoma differentiation-associated protein 5 (MDA5), which is encoded by the SMS-causative gene, is localized in dental pulp cells, periodontal ligaments, alveolar osteoblasts, odontoblasts, and ameloblasts (Ji et al., 2022; Rutsch et al., 2015). In addition, recent cell death studies have suggested that IFN type I may be involved in apoptotic and necroptotic cell death (Andzinski et al., 2015; Huang et al., 2012; Liu et al., 2019; McComb et al., 2014; Porta et al., 2005; Sarhan et al., 2019; Takaoka et al., 2003). Therefore, this study used mesenchymal stem cells derived from extracted dental pulp to investigate the effects of IFN type I on osteoblastogenesis.

IFN type I consists of 12 human IFN-α subtypes, IFN-ω, IFN-κ, and IFN-β. Among them, IFN-α and IFN-β play crucial roles in antiviral activity (de Weerd et al., 2013; Ikushima et al., 2013; Ivashkiv & Donlin, 2014; Piehler et al., 2012; Wittling et al., 2021). In our pilot study, the addition of IFN-α2A, IFN-α2B, and IFN-β recombinant proteins to the osteoblast differentiation medium caused no significant changes in the substrate formation ability or osteoblast number in the IFN-α2A and IFN-α2B groups compared to the control group (data not shown). Moreover, IFN-β has a higher affinity for the IFN-α/β receptor (IFNAR) and is more potent than IFN-α in several biological assays (de Weerd

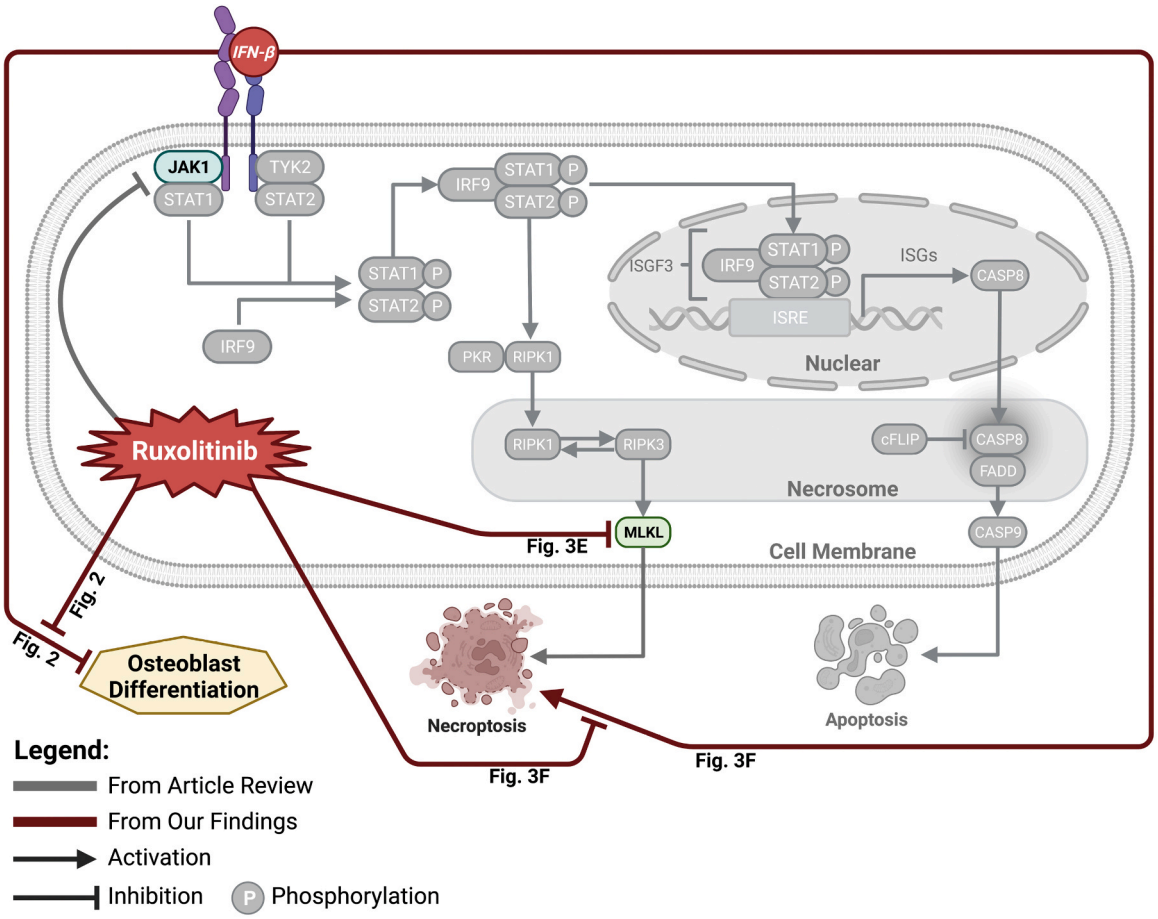

Fig. 4. Schematic diagram depicting our findings into a model of the IFN-β induced necroptosis during osteoblastogenesis via JAK-STAT pathway by reviewing articles (Ivashkiv & Donlin, 2014; Liu et al., 2019; McComb et al., 2014). According to the previous reports, in the activation of Canonical type I IFN signaling, STAT1 and STAT2 are phosphorylated and form the ISGF3 complex together with IRF9. Following translocation to the nucleus, the ISGF3 complex initiates the transcription of interferon-stimulated genes (ISGs) by binding to the ISRE regulatory sequence. The ISGs may eventually induce apoptosis through the CASP8/9 with the facilitation of cFLIP and FADD. On the other hand, ISGF3 may trigger the RIPK3-dependent necroptosis with the engagement of PKR and ROPK1 by regulating the conformational switch in MLKL. Our findings suggested that ruxolitinib interfered with the IFN-β-mediated osteoblast necroptosis and osteoblastogenesis via JAK-STAT pathway.

et al., 2013; Wittling et al., 2021). Thus, IFN-β may play a more important role in osteoblast differentiation. Therefore, IFN-β was the focus of this study.

The number of osteoblasts in the IFN-β-treated groups decreased (Fig. 1E) without changing the proliferative ability (Fig. 1A-C), suggesting that other factors may be important for this decrease. Gene expression analysis revealed that *CASP9* expression was significantly increased (Fig. 3C), and DNA fragmentation detected using TUNEL staining was slightly increased without statistical significance in the IFN-β-treated groups (Fig. 3A-B). In addition, a significant increase in *IL-6*, an inflammatory response marker that should not be increased in the apoptotic pathway, was observed in the IFN-β-treated groups (Fig. 3D). Furthermore, increased pMLKL expression was observed in the IFN-β-treated groups (Fig. 3E). These results suggest that IFN-β may cause necroptosis and apoptosis during osteoblast differentiation.

Furthermore, to determine the pathway by which IFN-β signaling induces necroptosis, ruxolitinib, a JAK1 and JAK2 inhibitor, was used to suppress the JAK-STAT pathway in IFN-β-treated osteoblasts. Ruxolitinib counteracted the IFN-β-induced increases of pMLKL and *IL-6* (Fig. 3C-E) and showed significant interaction effect with IFN-β (Table 2), suggesting that inhibiting the JAK-STAT pathway may neutralize IFN-β-induced necroptosis, consistent with previous reports that IFN-β induces apoptosis and necroptosis in tumor cells via the JAK-STAT pathway (Huang et al., 2012). Given the discussion above, our findings suggested that IFN-β treatment induced necroptosis via the JAK-STAT pathway, resulting in decreased osteoblast numbers (Fig. 4).

In contrast, ruxolitinib did not affect *CASP9* expression levels in the IFN-β-treated group, indicating that IFN-β induces *CASP9* through a non-JAK-STAT pathway. Therefore, further studies are required to understand the mechanism by which IFN-β regulates the apoptotic pathway (Fig. 4).

Furthermore, IFN-β suppressed the expression of *ALP*, an early-stage osteoblastogenic marker (Amarasekara et al., 2021), and promoted the expression of Osteocalcin, a mature osteoblast marker (Amarasekara et al., 2021) (Fig. 2C-E). In addition, ruxolitinib neutralized IFN-β-induced impairment of the expression of these osteoblast differentiation markers (Fig. 2C-E). The significant interaction effect between ruxolitinib and IFN-β was also detected in the expression of these osteoblast differentiation makers (Table 2). These findings suggest that the activation of the JAK-STAT pathway by IFN-β affects osteoblast differentiation. However, the underlying regulatory mechanism requires further investigation.

Overall, this study demonstrated that activated IFN-β impaired substrate formation by inducing apoptotic and necrotic cell death via the JAK-STAT pathway during osteoblastogenesis. These findings could be important for understanding the molecular mechanisms of dysostosis in patients with type I interferonopathies and will be beneficial for establishing pharmacological therapies for type I interferonopathies.

Funding

This research was supported by the Japan society for the promotion of science (JSPS) KAKEN grant 19K10381, 20K23081, 22K10245, and 22F22114.

CRediT authorship contribution statement

Atsuko Tanaka: Methodology, Investigation, Data curation, Formal analysis, Writing- Original draft preparation. **Satoru Hayano:** Conceptualization, Design, Methodology, Investigation, Data curation, Formal analysis, Visualization, Writing - Original draft preparation, Writing - Reviewing and Editing, Project administration, Resources, Funding acquisition. **Masayo Nagata:** Data curation. **Takahiro Kosami:** Data curation. **Ziyi Wang:** Data curation, Formal analysis, Visualization, Writing - Reviewing and Editing, Resources. **Hiroshi Kamioka:** Writing - Reviewing and Editing, Supervision, Project administration, Resources, Funding acquisition.

Declaration of Competing Interest

None.

Acknowledgments

The authors are grateful to the patients for their participation in the study.

Appendix A. Supporting information

Supplementary data associated with this article can be found in the online version at doi:10.1016/j.archoralbio.2023.105797.

References

Amarasekara, D. S., Kim, S., & Rho, J. (2021). Regulation of osteoblast differentiation by cytokine networks. *International Journal of Molecular Sciences, 22*(6), 2851. https://doi.org/10.3390/ijms22062851

Amarasekara, D. S., Yun, H., Kim, S., Lee, N., Kim, H., & Rho, J. (2018). Regulation of osteoclast differentiation by cytokine networks. *Immune Network, 18*(1), Article e8. https://doi.org/10.4110/in.2018.18.e8

Andzinski, L., Wu, C. F., Lienenklaus, S., Kröger, A., Weiss, S., & Jablonska, J. (2015). Delayed apoptosis of tumor associated neutrophils in the absence of endogenous IFN-β. *International Journal of Cancer, 136*(3), 572–583. https://doi.org/10.1002/ijc.28957

Blanca, M. J., Alarcón, R., & Arnau, J. (2017). Non-normal data: Is ANOVA still a valid option? *Psicothema, 29*(4), 552–557. https://doi.org/10.7334/psicothema2016.383

Briggs, T. A., Rice, G. I., Daly, S., Urquhart, J., Gornall, H., Bader-Meunier, B., Baskar, K., Baskar, S., Baudouin, V., Beresford, M. W., Black, G. C., Dearman, R. J., de Zegher, F., Foster, E. S., Francès, C., Hayman, A. R., Hilton, E., Job-Deslandre, C., Kulkarni, M. L., Le Merrer, M., & Crow, Y. J. (2011). Tartrate-resistant acid phosphatase deficiency causes a bone dysplasia with autoimmunity and a type I interferon expression signature. *Nature Genetics, 43*(2), 127–131. https://doi.org/10.1038/ng.748

Broser, P., Von Mengershausen, U., Heldt, K., Bartholdi, D., Braun, D., Wolf, C., & Lee-Kirsch, M. A. (2022). Precision treatment of Singleton Merten syndrome with ruxolitinib: A case report. *Pediatric Rheumatology, 20*(1), 24. https://doi.org/10.1186/s12969-022-00686-7

Crow, Y. J. (2011). Type I interferonopathies: A novel set of inborn errors of immunity. *Annals of the New York Academy of Sciences, 1238*, 91–98. https://doi.org/10.1111/j.1749-6632.2011.06220.x

D'Arcy, M. S. (2019). Cell death: A review of the major forms of apoptosis, necrosis and autophagy. *Cell Biology International, 43*(6), 582–592. https://doi.org/10.1002/cbin.11137

de Weerd, N. A., Vivian, J. P., Nguyen, T. K., Mangan, N. E., Gould, J. A., Braniff, S. J., Zaker-Tabrizi, L., Fung, K. Y., Forster, S. C., Beddoe, T., Reid, H. H., Rossjohn, J., & Hertzog, P. J. (2013). Structural basis of a unique interferon-β signaling axis mediated via the receptor IFNAR1. *Nature immunology, 14*(9), 901–907. https://doi.org/10.1038/ni.2667

Gronthos, S., Mankani, M., Brahim, J., Robey, P. G., & Shi, S. (2000). Postnatal human dental pulp stem cells (DPSCs) in vitro and in vivo. *Proceedings of the National Academy of Sciences of the United States of America, 97*(25), 13625–13630. https://doi.org/10.1073/pnas.240309797

Haanen, C., & Vermes, I. (1995). Apoptosis and inflammation. *Apoptosis and Inflammation, 4*, 5–15. https://doi.org/10.1155/S0962935195000020

Huang, H., Xiao, T., He, L., Ji, H., & Liu, X. Y. (2012). Interferon-β-armed oncolytic adenovirus induces both apoptosis and necroptosis in cancer cells. *Acta Biochimica et Biophysica Sinica, 44*(9), 737–745. https://doi.org/10.1093/abbs/gms060

Ikushima, H., Negishi, H., & Taniguchi, T. (2013). The IRF family transcription factors at the interface of innate and adaptive immune responses. *Cold Spring Harbor Symposia on Quantitative Biology, 78*, 105–116. https://doi.org/10.1101/sqb.2013.78.020321

Islam, T. U., & Abbas, E. (2022). *Validity of ANOVA under Non-normality & Heterogeneity [Preprint]. In Review*. https://doi.org/10.21203/rs.3.rs-2071136/v1

Ivashkiv, L. B., & Donlin, L. T. (2014). Regulation of type I interferon responses. *Nature Reviews Immunology, 14*(1), 36–49. https://doi.org/10.1038/nri3581

Ji, X., Zhang, L., Yang, F., & Huang, D. (2022). Innate immune sensing of nucleic acid in endodontic infection. *International Endodontic Journal, 55*(12), 1335–1346. https://doi.org/10.1111/iej.13831

Karsenty, G., Kronenberg, H. M., & Settembre, C. (2009). Genetic control of bone formation. *Annual Review of Cell and Developmental Biology, 25*(1), 629–648. https://doi.org/10.1146/annurev.cellbio.042308.113308

Kaur, A., & Kumar, R. (2015). Comparative analysis of parametric and non-parametric tests. *Journal of Computer and Mathematical Sciences, 6*(6), 336–342.

Kawanabe, N., Fukushima, H., Ishihara, Y., Yanagita, T., Kurosaka, H., & Yamashiro, T. (2015). Isolation and characterization of SSEA-4-positive subpopulation of human deciduous dental pulp cells. *Clinical Oral Investigations, 19*(2), 363–371. https://doi.org/10.1007/s00784-014-1260-z

Kawanabe, N., Murata, S., Fukushima, H., Ishihara, Y., Yanagita, T., Yanagita, E., Ono, M., Kurosaka, H., Kamioka, H., Itoh, T., Kuboki, T., & Yamashiro, T. (2012). Stage-specific embryonic antigen-4 identifies human dental pulp stem cells. *Experimental Cell Research, 318*(5), 453–463. https://doi.org/10.1016/j.yexcr.2012.01.008

Kishimoto, T. (1989). The biology of interleukin-6. *Blood, 74*(1), 1–10.

Krajewski, S., Krajewska, M., Ellerby, L. M., Welsh, K., Xie, Z., Deveraux, Q. L., Salvesen, G. S., Bredesen, D. E., Rosenthal, R. E., & Fiskum, G. (1999). Release of caspase-9 from mitochondria during neuronal apoptosis and cerebral ischemia. *Proceedings of the National Academy of Sciences, 96*(10), 5752–5757. https://doi.org/10.1073/pnas.96.10.5752

Li, P., Zhou, L., Zhao, T., Liu, X., Zhang, P., Liu, Y., Zheng, X., & Li, Q. (2017). Caspase-9: structure, mechanisms and clinical application. *Oncotarget, 8*(14), 23996. https://doi.org/10.18632/oncotarget.15098

Liao, J., Huang, Y., Wang, Q., Chen, S., Zhang, C., Wang, D., Lv, Z., Zhang, X., Wu, M., & Chen, G. (2022). Gene regulatory network from cranial neural crest cells to osteoblast differentiation and calvarial bone development. *Cellular and Molecular Life Sciences, 79*(3), 158. https://doi.org/10.1007/s00018-022-04208-2

Liu, Y., Liu, T., Lei, T., Zhang, D., Du, S., Girani, L., Qi, D., Lin, C., Tong, R., & Wang, Y. (2019). RIP1/RIP3-regulated necroptosis as a target for multifaceted disease therapy. *International Journal of Molecular Medicine, 44*(3), 771–786. https://doi.org/10.3892/ijmm.2019.4244

Lu, C., & MacDougall, M. (2017). RIG-I-Like receptor signaling in singleton-merten syndrome. *Frontiers in Genetics, 8*, 118. https://doi.org/10.3389/fgene.2017.00118

McComb, S., Cessford, E., Alturki, N. A., Joseph, J., Shutinoski, B., Startek, J. B., Gamero, A. M., Mossman, K. L., & Sad, S. (2014). Type-I interferon signaling through ISGF3 complex is required for sustained Rip3 activation and necroptosis in macrophages. *Proceedings of the National Academy of Sciences, 111*(31), E3206–E3213. https://doi.org/10.1073/pnas.1407068111

Melki, I., & Frémond, M.-L. (2020). Type I interferonopathies: From a novel concept to targeted therapeutics. *Current Rheumatology Reports, 22*, 1–14. https://doi.org/10.1007/s11926-020-00909-4

Miura, M., Gronthos, S., Zhao, M., Lu, B., Fisher, L. W., Robey, P. G., & Shi, S. (2003). SHED: Stem cells from human exfoliated deciduous teeth. *Proceedings of the National Academy of Sciences, 100*(10), 5807–5812. https://doi.org/10.1073/pnas.0937635100

Munoz, J., Marque, M., Dandurand, M., Meunier, L., Crow, Y.-J., & Bessis, D. (2015). Interféronopathies de type I. *Annales Délelőtt Dermatologie et Délelőtt Vénéréologie, 142*(11), 653–663. https://doi.org/10.1016/j.annder.2015.06.018

Nikoletopoulou, V., Markaki, M., Palikaras, K., & Tavernarakis, N. (2013). Crosstalk between apoptosis, necrosis and autophagy. *Biochimica et Biophysica Acta (BBA)-Molecular Cell Research, 1833*(12), 3448–3459. https://doi.org/10.1016/j.bbamcr.2013.06.001

O'Shea, J. J., Schwartz, D. M., Villarino, A. V., Gadina, M., McInnes, I. B., & Laurence, A. (2015). The JAK-STAT pathway: Impact on human disease and therapeutic intervention. *Annual Review of Medicine, 66*(1), 311–328. https://doi.org/10.1146/annurev-med-051113-024537

Pettersson, M., Bergendal, B., Norderyd, J., Nilsson, D., Anderlid, B., Nordgren, A., & Lindstrand, A. (2017). Further evidence for specific IFIH1 mutation as a cause of Singleton–Merten syndrome with phenotypic heterogeneity. *American Journal of Medical Genetics Part A, 173*(5), 1396–1399. https://doi.org/10.1002/ajmg.a.38214

Piehler, J., Thomas, C., Garcia, K. C., & Schreiber, G. (2012). Structural and dynamic determinants of type I interferon receptor assembly and their functional interpretation. *Immunological Reviews, 250*(1), 317–334. https://doi.org/10.1111/imr.12001

Porta, C., Hadj-Slimane, R., Nejmeddine, M., Pampin, M., Tovey, M. G., Espert, L., Alvarez, S., & Chelbi-Alix, M. K. (2005). Interferons α and γ induce p53-dependent and p53-independent apoptosis, respectively. *Oncogene, 24*(4), 605–615. https://doi.org/10.1038/sj.onc.1208204

Qian, Z. Y., Kong, R. Y., Zhang, S., Wang, B. Y., Chang, J., Cao, J., Wu, C. Q., Huang, Z. Y., Duan, A., Li, H. J., Yang, L., & Cao, X. J. (2022). Ruxolitinib attenuates secondary injury after traumatic spinal cord injury. *Neural regeneration Research, 17*(9), 2029–2035. https://doi.org/10.4103/1673-5374.335165

Rice, G. I., del Toro Duany, Y., Jenkinson, E. M., Forte, G. M., Anderson, B. H., Ariaudo, G., Bader-Meunier, B., Baildam, E. M., Battini, R., & Beresford, M. W. (2014). Gain-of-function mutations in IFIH1 cause a spectrum of human disease phenotypes associated with upregulated type I interferon signaling. *Nature Genetics, 46*(5), 503–509. https://doi.org/10.1038/ng.2933

Rice, G. I., Park, S., Gavazzi, F., Adang, L. A., Ayuk, L. A., Van Eyck, L., Seabra, L., Barrea, C., Battini, R., Belot, A., Berg, S., Billette De Villemeur, T., Bley, A. E., Blumkin, L., Boespflug-Tanguy, O., Briggs, T. A., Brimble, E., Dale, R. C., Darin, N., & Crow, Y. J. (2020). Genetic and phenotypic spectrum associated with IFIH1 gain-of-function. *Human Mutation, 41*(4), 837–849. https://doi.org/10.1002/humu.23975

Rutsch, F., MacDougall, M., Lu, C., Buers, I., Mamaeva, O., Nitschke, Y., Rice, G. I., Erlandsen, H., Kehl, H. G., & Thiele, H. (2015). A specific IFIH1 gain-of-function mutation causes Singleton-Merten syndrome. *The American Journal of Human Genetics, 96*(2), 275–282. https://doi.org/10.1016/j.ajhg.2014.12.014

Sarhan, J., Liu, B. C., Muendlein, H. I., Weindel, C. G., Smirnova, I., Tang, A. Y., Ilyukha, V., Sorokin, M., Buzdin, A., & Fitzgerald, K. A. (2019). Constitutive interferon signaling maintains critical threshold of MLKL expression to license necroptosis. *Cell Death & Differentiation, 26*(2), 332–347. https://doi.org/10.1038/s41418-018-0122-7

Schwartz, L. M., & Osborne, B. A. (1993). Programmed cell death, apoptosis and killer genes. *Immunology Today, 14*(12), 582–590. https://doi.org/10.1016/0167-5699(93)90197-S

Shakeri, R., Kheirollahi, A., & Davoodi, J. (2017). Apaf-1: Regulation and function in cell death. *Biochimie, 135*, 111–125. https://doi.org/10.1016/j.biochi.2017.02.001

Shi, Y. (2002). Mechanisms of caspase activation and inhibition during apoptosis. *Molecular Cell, 9*(3), 459–470. https://doi.org/10.1016/s1097-2765(02)00482-3

Su, Z., Yang, Z., Xu, Y., Chen, Y., & Yu, Q. (2015). Apoptosis, autophagy, necroptosis, and cancer metastasis. *Molecular Cancer, 14*, 1–14. https://doi.org/10.1186/s12943-015-0321-5

Takaoka, A., Hayakawa, S., Yanai, H., Stoiber, D., Negishi, H., Kikuchi, H., Sasaki, S., Imai, K., Shibue, T., Honda, K., & Taniguchi, T. (2003). Integration of interferon-alpha/beta signalling to p53 responses in tumour suppression and antiviral defence. *Nature, 424*(6948), 516–523. https://doi.org/10.1038/nature01850

Takayanagi, H., Kim, S., Matsuo, K., Suzuki, H., Suzuki, T., Sato, K., Yokochi, T., Oda, H., Nakamura, K., Ida, N., Wagner, E. F., & Taniguchi, T. (2002). RANKL maintains bone homeostasis through c-Fos-dependent induction of interferon-beta. *Nature, 416*(6882), 744–749. https://doi.org/10.1038/416744a

Wittling, M. C., Cahalan, S. R., Levenson, E. A., & Rabin, R. L. (2021). Shared and unique features of human interferon-beta and interferon-alpha subtypes. *Frontiers in Immunology, 11*, Article 605673. https://doi.org/10.3389/fimmu.2020.605673

Xu, X., Lai, Y., & Hua, Z. C. (2019). Apoptosis and apoptotic body: Disease message and therapeutic target potentials. *Bioscience Reports, 39*(1), Article BSR20180992. https://doi.org/10.1042/BSR20180992